

# Lidar-based Obstacle Avoidance for the Autonomous Mobile Robot

Dony Hutabarat

*Department of Electrical Engineering  
Institut Teknologi Sepuluh Nopember  
Surabaya, Indonesia  
donyhutabarat.18071@mhs.its.ac.id*

Djoko Purwanto

*Department of Electrical Engineering  
Institut Teknologi Sepuluh Nopember  
Surabaya, Indonesia  
djoko@ee.its.ac.id*

Muhammad Rivai

*Department of Electrical Engineering  
Institut Teknologi Sepuluh Nopember  
Surabaya, Indonesia  
muhammad\_rivai@ee.its.ac.id*

Harjuno Hutomo

*Department of Electrical Engineering  
Institut Teknologi Sepuluh Nopember  
Surabaya, Indonesia  
harjuno270396@gmail.com*

**Abstract**— In conditions that are dangerous for humans and their environment, the use of robots can be a solution to overcome these problems. Various sensors are used to determine the obstacle free path and the exact position of the robot. However, conventional sensors have limitations in terms of detection distance, spatial resolution, and processing complexity. In this study, an autonomous mobile robot has been developed equipped with Light Detection and Ranging (LiDAR) sensor to avoid obstacle. Braitenberg vehicle strategy is used to navigate the movements of the robot. Sensor data collection and control algorithm are implemented on a single computer board of Raspberry Pi 3. The experimental results show that this sensor can measure distance consistently which is not affected by the object's color and ambient light intensity. The mobile robot can avoid colored objects of different sizes. This autonomous mobile robot can also navigate inside a room without any impact on the wall or the obstacle.

**Keywords** —Autonomous mobile robot, Braitenberg vehicle, LiDAR, Obstacle avoidance

## I. INTRODUCTION

Some dangerous situations, such as chemical industries, polluted environments, and mining areas can endanger workers and residents around them. These will have an impact on both financial and life losses. Therefore, the use of robots can be a solution to overcome these problems [1]. Mobile robots equipped with several sensors can investigate in a room or in an open area [2], as well as in industrial fields [3, 4]. The autonomous mobile robots that have been developed are equipped with obstacle avoidance features as one type of intelligent robots [5].

The ability to detect walls and obstacles around them to predict collision-free paths automatically is the main feature of autonomous mobile robots [6]. Various sensors such as infrared and ultrasonic range finders, cameras and GPS are used to determine the obstacle free path and the exact position of the mobile robot [7]. However, these conventional sensors have limitations in terms of detection distance, spatial resolution, and processing complexity. As an instance, blanking intervals and angular uncertainty are limitations on the ultrasonic distance sensors [8].

In this study, Light Detection and Ranging (LiDAR) technology is used as an obstacle avoidance system on an autonomous mobile robot. LiDAR has several advantages,

such as a high level of precision with a long detection distance [5,7].

## II. LITERATURE REVIEW

### A. Light Detection and Ranging

LiDAR is an optical scanning technology that measures the properties of radiated light to find distance and other information from target. Shooting pulses of laser light onto the object's surface is one method for determining the distance of an object, as shown in Figure 1. Light travels at a speed of about 300,000 kilometers per second or 0.3 meters per nanosecond in vacuum. The time difference between light emitted and received back can be used to determine the distance of the object [9-11].

The standard information from LiDAR is an arrangement of points on polar coordinates [8]. The distance measuring technology is widely used in the fields of geodesy, archeology, geography, geology, geomorphology, seismology, and remote sensing [12]. In this study, we use X4 YDLiDAR, a LiDAR which is equipped with a motor so that it can rotate to provide a 360-degree view, which has a working voltage of 5 V and a range of measurements from 0.12 m to 10 m indoors. The interface data communication uses a serial port or USB adapter.

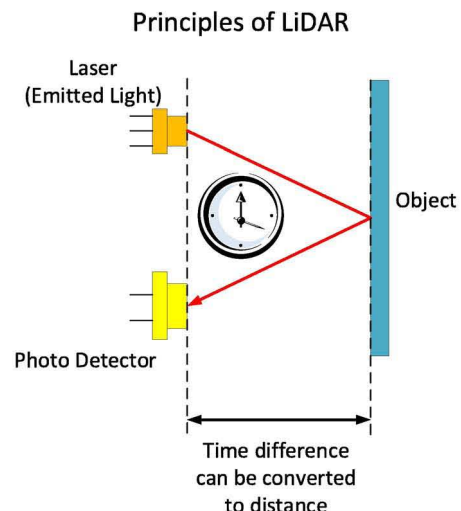


Fig. 1. The principles of LiDAR.

## B. Raspberry Pi

Raspberry Pi is a single board computer that can be used in various applications. Raspberry Pi 3 works at a voltage of 5V using a micro USB connector. This computer uses the Broadcom BCM287 chip set processor, with 1 GB of memory, as shown in Table 1. Raspberry Pi has data storage of a SD card memory, as shown in Figure 2.

Table 1. Raspberry Pi 3 technical specifications [13].

Microprocessor	Broadcom BCM2837 64 bit Quad Core Processor
Processor Operating Voltage	3.3V
Raw Voltage input	5 V, 2 A power source
Maximum current through each I/O pin	16 mA
Maximum total current drawn from all I/O pins	54 mA
Flash Memory (Operating System)	16 Gbytes SSD memory card
Internal RAM	1 G bytes DDR2
Clock Frequency	1.2 GHz
GPU	Dual Core Video Core IV® Multimedia Co-Processor. Provides Open GLES 2.0, hardware-accelerated Open VG, and 1080p30 H.264 high-profile decode. Capable of 1Gpixel/s, 1.5Gtexel/s or 24GFLOPs with texture filtering and DMA infrastructure.
Ethernet	10/100 Ethernet
Wireless Connectivity	BCM43143 (802.11 b/g/n Wireless LAN and Bluetooth 4.1)
Operating Temperature	-40 °C to +85 °C

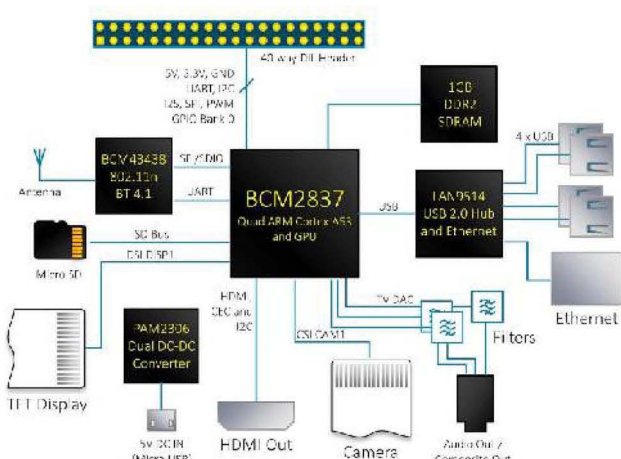


Fig. 2. Block diagram of the Raspberry Pi 3 [14].

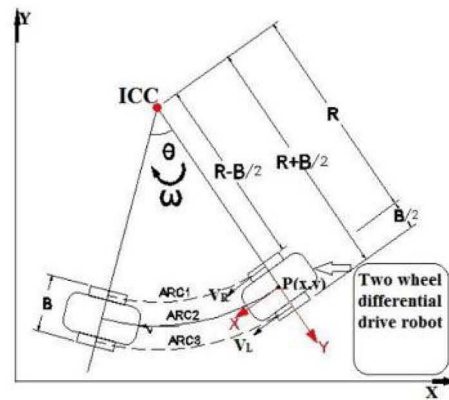


Fig. 3. The differential drive kinematics model [12].

## C. Mobile Robot

Many kinds of sensors can be implemented on a mobile robot to determine its environmental conditions. The sensors commonly used are ultrasonic, infrared, camera, and others [15]. In this study, a LiDAR sensor is implemented on a differential drive mobile robot, where there are two wheels each of which is driven by a dc motor and a free wheel [16].

The difference in speed between the right and left wheels is used as a robot control in this steering type [15,17,18]. The speed difference will result in a kinematic motion of the mobile robot that forms a rotating angle when the mobile robot turns the direction. The kinematics model for differential steering is shown in Figure 3, where the ICC is the Instantaneous Center of Curvature, R is the radius of the ICC to the midpoint between two robot wheels, B is the width of the robot, VR is the linear speed of the right wheel, VL is the linear speed of left wheel. The relationship between linear and angular velocity is as follows:

$$V = \omega R \quad (1)$$

$$V_L = \omega * \left( R + \frac{B}{2} \right) \quad (2)$$

$$V_R = \omega * \left( R - \frac{B}{2} \right) \quad (3)$$

## D. Braitenberg Vehicle

Braitenberg vehicle is a vehicle which is equipped with two sensors and two motors, but with different connections between them [19]. Figure 4 shows the type of braitenberg vehicle 2a and 2b. The Braitenberg vehicle 2a is the type used for obstacle avoidance, while type 2b is for tracking. The '+' sign indicates a higher sensor signal which will increase the dc motor speed.

In the Braitenberg algorithm, a number of sensors are connected to motor settings where the motor speed is affected by the sensor input [20]. The algorithm produces a weighted matrix that converts sensor inputs into motor speeds. The matrix is a two-dimensional array with the columns and the rows are the number of sensors, and the number of motors, respectively.

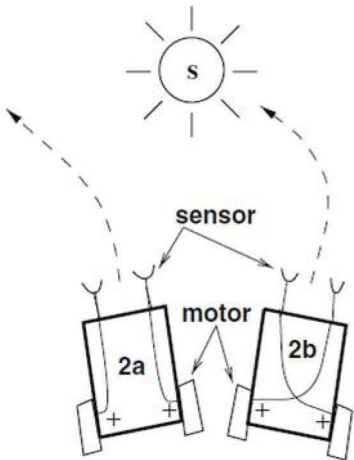


Fig. 4. Braatenberg vehicle 2a dan 2b [16].

Equation (4) represents the weighted matrix with  $W_{LS1}$  is the value of the  $S_1$  sensor to adjust the left motor speed, while equation (5) is the value of the sensor. The motor speed can be calculated as shown in equation (6), where  $S_{\max}$  is the maximum value of sensor.

$$W_R = \begin{bmatrix} W_{LS_1} & \dots & W_{LS_n} \\ W_{RS_1} & \dots & W_{RS_n} \end{bmatrix} \quad (4)$$

$$S = [S_1 \quad \dots \quad S_n]^T \quad (5)$$

$$v_{L,R} = W * (1 - (S / S_{\max})) \quad (6)$$

### III. RESEARCH METHODS

Figure 5 depicts the overall block diagram of the obstacle avoidance system. The values that will be used as the references in this system are the coordinates of the angle and distance of the object obtained from LiDAR. Robot Operating System (ROS) and YDLiDAR drivers are installed on the Raspberry Pi 3 single computer board. This study applies the Braatenberg vehicle 2b method where the sensor on the left side of the mobile robot is used to control the right motor and vice versa. Pulse Width Modulation (PWM) method is used to determine the motor speed.

Figure 6 shows the LiDAR which acts as a sensor that scans the distance of object in a clockwise direction. In this study, only 360 data will be used in the range from  $90^\circ$  to  $-90^\circ$  for a half-degree change. The weight values and the results of distance measurements can be presented in equation (7) and (8), respectively. Equation (9) and (10) are used to adjust the motor speed, with  $v_{\max}$  is the motor speed when PWM at the duty cycle of 100%,  $d_{\min}$  of 0.15 is the minimum distance value, and  $d_{\max}$  of 0.5 is the maximum distance value.

$$W_L = [W_{RL_1} \quad \dots \quad W_{RL_2}] \quad (7)$$

$$W_R = [W_{Rd_1} \quad \dots \quad W_{Rd_2}] \quad (7)$$

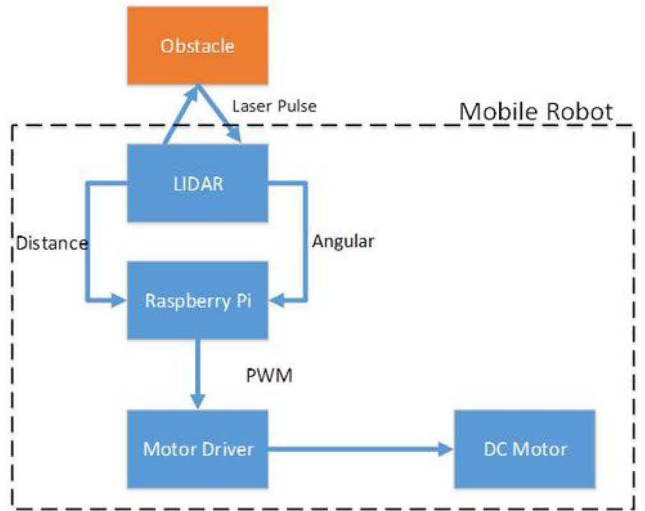


Fig. 5. Block diagram of the mobile robot system.

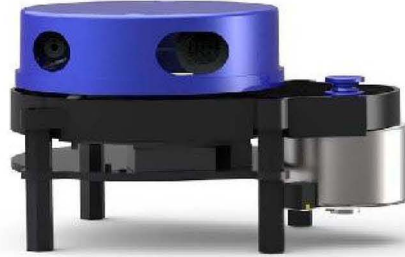


Fig. 6. The YDLIDAR X4 with 360° scanning [21].

$$d = [d_1 \quad \dots \quad d_{360}]^T \quad (8)$$

$$v_L = v_{\max} - \left( W_L * \left( 1 - \left( \frac{d - d_{\min}}{d_{\max} - d_{\min}} \right) \right) \right) \quad (9)$$

$$v_R = v_{\max} - \left( W_R * \left( 1 - \left( \frac{d - d_{\min}}{d_{\max} - d_{\min}} \right) \right) \right) \quad (10)$$

If the distance is less than 0.5 m at an angle between  $90^\circ$  and  $0^\circ$ , then the right motor speed will gradually decrease until the distance is 0.15 m. The motor speed reaches a minimum and makes the robot turn right, and vice versa. The flow diagram of the obstacle avoidance system is shown in Figure 7.

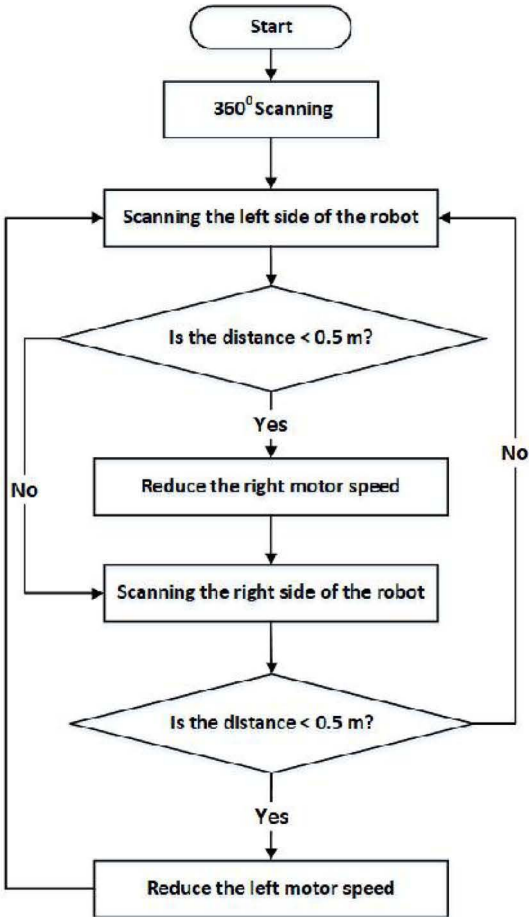


Fig. 7. Flowchart of the obstacle avoidance system.

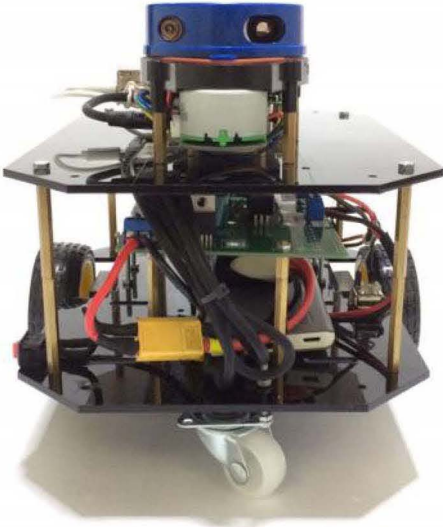


Fig. 8. The mobile robot platform used in this experiment.

#### IV. RESULTS AND DISCUSSION

##### A. LiDAR measurement

The mobile robot platform used in this experiment is shown in Figure 8. The robot consists of LiDAR as a 360 scanner sensor for obtaining the angle and distance of objects around robot, Raspberry Pi 3 as a data collector from LiDAR and as a motor controller, motor driver module, 11.1V

Lithium Polymer (LiPo) battery pack, and Buck converter step down module as a 5V power supply. Table 2 shows that the minimum and maximum distance measurements of the LiDAR are 0.12 m and 10.5 m, respectively, with an average error of 0.9%. In order to find out the reliability of the data obtained by the LiDAR, the measurements are carried out with various environmental light intensities and different object colors. There are six kinds of object colors in each of the experiment, namely red, green, blue, orange, purple, and black, with the object distances of 1m and 2m. The results of LiDAR measurements for light intensity of 83 lux, 15.5 lux, and 0.04 lux are shown in Table 3, Table 4, and Table 5, respectively. The results of this experiment shows that the ambient light intensity and the surface color of the object do not significantly influence the LiDAR measurements.

Table 2. The LiDAR measurements.

Distance (m)	Read Distance (m)	Error (%)
0 – 0.11	0	-
0.12	0.121	0.83
0.16	0.161	0.83
0.20	0.201	0.83
0.24	0.241	0.83
0.5	0.505	1
1.5	1.495	0.33
2.5	2.509	0.36
3.5	3.517	0.48
4.5	4.531	0.68
5.5	5.525	0.45
6.5	6.561	0.93
7.5	7.606	1.41
8.5	8.600	1.17
9.5	9.679	1.88
10.5	10.662	1.54
11.5	0	-
12.5	0	-
<b>Average</b>	<b>0.9</b>	

Table 3. The LiDAR measurements at a light intensity of 83 lux.

Object Color	Object distance: 1 m		Object distance: 2 m	
	Measured distance (m)	Error (%)	Measured distance (m)	Error (%)
Red	0.994	0.6	2.016	0.8
Green	0.984	1.6	2.008	0.4
Blue	0.980	2	2.013	0.65
Orange	0.992	0.8	2.006	0.3
Purple	0.991	0.9	2.001	0.05
Black	1.003	0.3	2.033	1.65
<b>Average</b>	<b>0.990</b>	<b>1.03</b>	<b>2.013</b>	<b>0.64</b>

Table 4. The LiDAR measurements at a light intensity of 15.5 lux.

Object Color	Object distance: 1 m		Object distance: 2 m	
	Measured distance (m)	Error (%)	Measured distance (m)	Error (%)
Red	0.992	0.8	2.099	0.49
Green	0.991	0.9	2.091	0.45
Blue	0.992	0.8	2.069	0.34
Orange	0.980	2	2.005	0.25
Purple	0.991	0.9	2.088	0.44
Black	1.003	0.3	2.022	1.1
Average	<b>0.991</b>	<b>0.95</b>	<b>2.062</b>	<b>0.51</b>

Table 5. The LiDAR measurements at a light intensity of 0.04 lux.

Object Color	Object distance: 1 m		Object distance: 2 m	
	Measured distance (m)	Error (%)	Measured distance (m)	Error (%)
Red	0.992	0.8	2.013	0.65
Green	0.993	0.7	1.978	1.1
Blue	0.983	1.7	1.994	0.3
Orange	0.991	0.9	1.982	0.9
Purple	0.995	0.5	1.990	0.5
Black	1.002	0.2	2.018	0.9
Average	<b>0.992</b>	<b>0.80</b>	<b>1.996</b>	<b>0.72</b>

Table 6. The mobile robot avoidance to various obstacle colors.

Object Color	Object distance: 25 cm		Object distance: 50 cm	
	Collisions		Collisions	
	Yes	No	Yes	No
Red		✓		✓
Green		✓		✓
Blue		✓		✓
Orange		✓		✓
Purple		✓		✓
Black		✓		✓
Total (%)	<b>0</b>	<b>100</b>	<b>0</b>	<b>100</b>

Table 7. The mobile robot avoidance to various obstacle widths.

Object Width (cm)	Object distance: 25 cm		Object distance: 50 cm	
	Collisions		Collisions	
	Yes	No	Yes	No
5		✓		✓
10		✓		✓
15		✓		✓
20		✓		✓
25		✓		✓
30		✓		✓
Total (%)	<b>0</b>	<b>100</b>	<b>0</b>	<b>100</b>

### B. Avoidance of the mobile robot to various obstacles

In the first experiment, avoidance of the mobile robot is carried out with various obstacle colors with the distances of 25 cm and 50 cm. Table 6 shows that the mobile robot can avoid various colors of object with a success rate of 100%. In the second experiment, avoidance of the mobile robot is carried out with various obstacle widths with the distances of 25 cm and 50 cm. Table 7 shows that the mobile robot can avoid various widths of object with a success rate of 100%. The third experiment is carried out with various colors and sizes of obstacle with the distances of 25cm and 50cm. Table 8 shows that the mobile robot can avoid colored objects of different sizes, namely glass bottle, jerry can, and cardboard box. However, the robot cannot avoid transparent objects such as acrylic and polycarbonate bottle. This can be caused by the laser pulses emitted by LiDAR do not reflected back by the object. The overall experiment includes a navigation of the autonomous mobile robot through an indoor room both with and without obstacle. The results of the two experiments show that the mobile robot manages to navigate the room without hitting or crashing into the wall or obstacle. The movements of the mobile robot are shown in Figure 9 and Figure 10.

Table 8. The mobile robot avoidance to various obstacles.

Object	Object distance: 25 cm		Object distance: 50 cm	
	Collisions		Collisions	
	Yes	No	Yes	No
Acrylic	✓		✓	
Polycarbonate Bottle	✓		✓	
Glass Bottle			✓	
Jerry cans			✓	
Cardboard			✓	

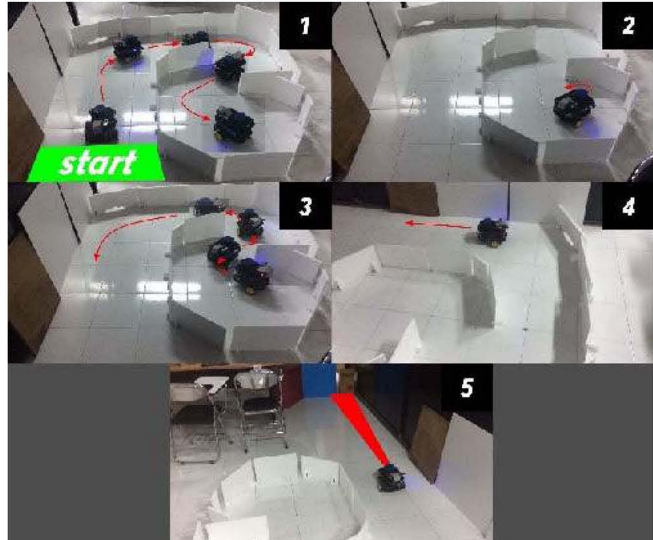


Fig. 9. The mobile robot navigation in a room without obstacle.

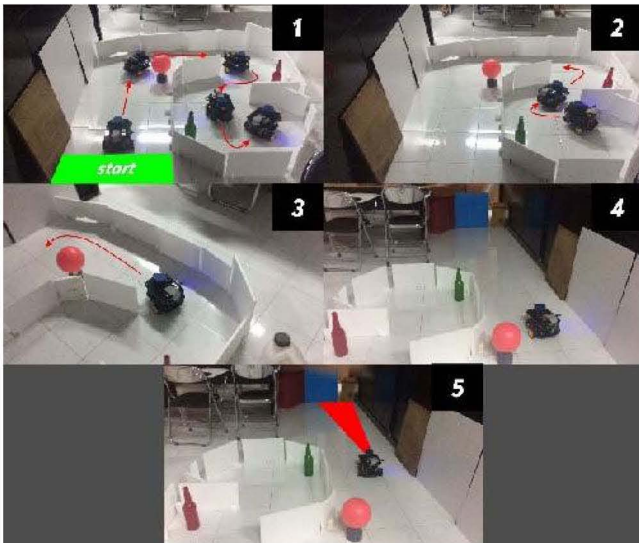


Fig. 10. The mobile robot navigation in a room with obstacle.

## V. CONCLUSION

In this study, a differential drive autonomous mobile robot equipped with LiDAR has been developed to avoid obstacle. The Braatenberg vehicle strategy is used to navigate the movements of the robot. The distance measurements and the control algorithm are implemented on a single board computer of Raspberry Pi 3. The experimental results show that LiDAR can measure distances between 0.12 to 10.5 m with an error rate of 0.9%. The color of the object and the intensity of ambient light do not affect the measurements obtained from LiDAR. The autonomous mobile robot can avoid colored objects of different sizes. However, the robot cannot avoid transparent objects. This autonomous mobile robot can navigate indoor room both with and without obstacle with no impact on wall or obstacle.

## ACKNOWLEDGMENT

This research was carried out with financial aid support from the Ministry of Research, Technology and Higher Education of the Republic of Indonesia (Kemenristekdikti RI).

## REFERENCES

- [1] M. Vuka, E. Schaffernicht, M. Schmuker, V. H. Bennetts, F. Amigoni, A. J. Lilienthal, "Exploration and localization of a gas source with MOX gas sensors on a mobile robot-A Gaussian regression bout amplitude approach", ISOEN - ISOCS/IEEE Int. Symp. Olfaction Electron. Nose, 2017, pp. 3–5.
- [2] H. Widyantara, M. Rivai, D. Purwanto, "Wind direction sensor based on thermal anemometer for olfactory mobile robot", Indonesian Journal of Electrical Engineering and Computer Science, vol. 13, no. 2, 2019, pp. 475–484.
- [3] M. Rivai, Rendyansyah, D. Purwanto, "Implementation of fuzzy logic control in robot arm for searching location of gas leak", International Seminar on Intelligent Technology and Its Application, 2015, pp. 69–74.
- [4] G. A. Rahardi, M. Rivai, D. Purwanto, "Implementation of hot-wire anemometer on olfactory mobile robot to localize gas source", International Conference on Information and Communications Technology, 2018, pp. 412–417.
- [5] Y. Peng, D. Qu, Y. Zhong, S. Xie, J. Luo, J. Gu, "The obstacle detection and obstacle avoidance algorithm based on 2-D lidar", IEEE Int. Conf. Inf. Autom. ICIA - conjunction with IEEE Int. Conf. Autom. Logist., 2015, pp. 1648–1653.
- [6] M. Bengel, K. Pfeiffer, B. Graf, A. Bubeck, A. Verl, "Mobile robots for offshore inspection and manipulation", IEEE/RSJ Int. Conf. Intell. Robot. Syst., 2009, pp. 3317–3322.
- [7] K. H. Hsia, H. Guo, K. L. Su, "Motion guidance of mobile robot using laser range finder", iFUZZY- Int. Conf. Fuzzy Theory Its Appl., 2013, pp. 293–298.
- [8] N. A. Rahim, M. A. Markom, A. H. Adom, S. A. A. Shukor, A. Y. M. Shakaff, E. S. M. M. Tan, "A mapping mobile robot using RP Lidar scanner", 2016, pp. 87–92.
- [9] M. D. Adams, "Lidar design, use, and calibration concepts for correct environmental detection", IEEE Trans. Robot. Autom., vol. 16, no. 6, 2000, pp. 753–761.
- [10] M. M. Atia, S. Liu, H. Nematallah, T. B. Karamat, A. Noureldin, "Integrated indoor navigation system for ground vehicles with automatic 3-D alignment and position initialization", IEEE Trans. Veh. Technol., vol. 64, no. 4, 2015, pp. 1279–1292.
- [11] J. Liu, Q. Sun, Z. Fan, "TOF Lidar Development in Autonomous Vehicle", IEEE 3rd Optoelectron. Glob. Conf., 2018, pp. 185–190.
- [12] J. Zhang, S. Singh, "Visual-lidar odometry and mapping: Low-drift, robust, and fast", Proc. - IEEE Int. Conf. Robot. Autom., 2015, pp. 2174–2181.
- [13] "Raspberry Pi 3 Pinout, Features, Specifications & Datasheet," [Online]. Available: <https://components101.com/microcontrollers/raspberry-pi-3-pinout-features-datasheet>. [Accessed: 03-Jul-2019].
- [14] "pi3-block-diagram-rev4.png (1259×900)." [Online]. Available: <http://doc.xdevs.com/doc/RPi/pi3-block-diagram-rev4.png>. [Accessed: 03-Jul-2019].
- [15] M. S. Saidonr, H. Desa, M. N. Rudzuan, "A differential steering control with proportional controller for an autonomous mobile robot", Proc. IEEE 7th Int. Colloq. Signal Process. Its Appl. CSPA, 2011, pp. 90–94.
- [16] J. Singh, P. S. Chouhan, "A new approach for line following robot using radius of path curvature and differential drive kinematics", 6th Int. Conf. Comput. Appl. Electr. Eng. - Recent Adv. CERA, 2017, pp. 497–502.
- [17] R. Watiasih, M. Rivai, R. A. Wibowo, O. Penangsang, "Path planning mobile robot using waypoint for gas level mapping", International Seminar on Intelligent Technology and Its Application, 2017, pp. 244–249.
- [18] R. Watiasih, M. Rivai, O. Penangsang, F. Budiman, Tukadi, Y. Izza, "Online Gas Mapping in Outdoor Environment using Solar-Powered Mobile Robot", International Conference on Computer Engineering, Network and Intelligent Multimedia, 2018, pp. 245–250.
- [19] X. Yang, R. V. Patel, M. Moallem, "A fuzzy-braitenberg navigation strategy for differential drive mobile robots", J. Intell. Robot. Syst. Theory Appl., vol. 47, no. 2, 2006, pp. 101–124.
- [20] E. Fabregas, G. Farias, E. Peralta, H. Vargas, S. Dormido, "Teaching control in mobile robotics with V-REP and a Khepera IV library", IEEE Conf. Control Appl. CCA 2016, pp. 821–826.
- [21] "YDLIDAR X4 DATASHEET," 2015.